

Electronic Properties and Conformation Analysis of Phytochromobilins, Chromophore in Phytochrome

Cheol-Ju Kim* and Dong Jin Yoo†

Department of Chemistry, Chonbuk National University, Chonju 561-756, Korea. *E-mail: cjkim@chonbuk.ac.kr

†Department of Chemistry, Seonam University, Namwon 590-711, Korea

Received March 31, 2008

Quantum-chemical investigation on the conformation analysis and electronic properties of phytochromobilins (PCBs), an open chain tetrapyrrole chromophore of phytochrome are performed. The PCB chromophore have two stable forms, which occur photoisomerization by visible light absorption. Structures for two stable forms, **Pr** and **Pfr** isomers were fully optimized by using semiempirical AM1, PM3 methods, *ab initio* HF/3-21G(d), and B3LYP/6-31G(d) methods. The potential energy curves with respect to the change of single torsion angle are obtained by using semiempirical methods, *ab initio* HF, and DFT calculations. It is shown that the conformations of the isomers are compromised between the steric repulsion interaction and the degree of the conjugation. Electronic properties of the molecules were obtained by applying the optimized structures and geometries to the Zindo/S method. Absorption wavelengths are predicted by Zindo/S analysis. The wavelengths which are calculated from optimized geometries by HF/3-21G(d) and B3LYP/6-31G(d) is reported. The absorption wavelength on the optimized geometries by B3LYP/6-31G(d) is much longer than that by HF/3-21G(d) level. The absorption wavelengths of **Pfr** form are longer than that of corresponding **Pr** form in the same torsion angle because of conjugation length difference. The absorption wavelengths of isomers with perpendicular linkage are shorter than those of planar linkage.

Key Words : Conformation analysis, Potential energy curve, Phytochromobilins, Phytochrome, Electronic properties

Introduction

It is well-known that phytochrome is biliprotein photoreceptors of plants, fungi, and bacteria. Phytochromes allow these organisms to respond to environmental light conditions.¹⁻³ Organisms can use light in two ways. The one is to use its energy to keep its cells functioning, the other is to use to transduce optical signals into some kind of biological response. Like rhodopsin in vertebrates, phytochrome in higher plants converts long wavelength light energy into cellular signals inducing photomorphogenesis. The molecular basis of phytochrome action depends on the ability to convert between the stable isomers, the red light absorbing conformer, **Pr**, and the far-red light absorbing conformer of phytochrome **Pfr**. This physiological function is mediated via a light induced conversion of the parent state **Pr** form into the physiologically active state **Pfr**.⁴⁻⁷ The primary reaction of the conversion consists of photoisomerization of the chromophore, which is followed by a series of thermally driven conformational changes of protein and chromophore.

Even for the stable states, **Pr** and **Pfr**, the structure determination by X-ray crystallography and NMR spectroscopy is not possible due to the lack of crystals or due to protein size.⁸⁻¹⁰ Other spectroscopic techniques have been employed to investigate the structure and conformation of the chromophore. One of the techniques is resonance Raman (RR) spectroscopy, which can characterize the vibrational band pattern of the chromophore.^{15,16} Some studies are showed that RR spectra have been obtained from the stable

states, **Pr** and **Pfr** as well as from several intermediates formed during the reaction cycle.²

After the assembly of the apoprotein with the chromophore, phytochrome exists in a red light absorbing conformation (**Pr**). The absorption maximum of **Pr** form shows a peak around 660 nm.^{1,2,6} The chromophore, phytochromobilin (**PCB**) is covalently bound (formation of thioether bound a cystine residue) to the apoprotein. **PCB** is an open chain tetrapyrrolic chromophore (Fig. 1). Photoconversion is associated with very rapid isomerization around the C15-C16 double bond followed by a series of slower conformational changes in the dark. **PCB** changes its conformation via a *Z* → *E* isomerization, which brings protein into a different conformation, the far-red light absorbing form (**Pfr**). The absorption maximum of **Pfr** form shows a peak around 730 nm (Fig. 2).^{3,6}

Conformational studies of the chromophore have been performed by using *ab initio* and semiempirical studies of oligopyrrolic compounds and tetrapyrrole backbone.¹¹⁻¹⁴ The oligopyrrolic compounds like pyromethene and pyromethenone are important as a source of information about structure and electronic properties of the chromophore. The methenone molecule is adapted for model of non-hydrogen bonded part of the chromophore and the dipyrrolic pyromethene is utilized as a model of hydrogen bond part of the chromophore. It was reported that AM1 and the *ab initio* and (HF/6-31G(d) and MP2/6-31G(d)) methods are reliable results for conformational analysis.^{11,13} DHB (2,3-dihydrobilin-119(21H, 24H)-dione) was studied as a model of the

fully conjugated linear open chain tetrapyrroles. The geometries and energies of conformers were investigated with AM1 and HF/3-21G(d) level and the results of the two methods was indicated that the geometries were investigated with a central *syn-cis* configuration are preferred to other conformations around the central methine bridge.^{8,14-16} Conformation analysis in various metal-organic complex or oligomers in macromolecule are performed using *ab initio* calculation.^{20,31,32}

In this paper, **PCB** was chosen to investigate the effect of the conformations and electronic properties for conformational isomers, Pr, and Pfr, which are chromophore of phytochrome. The molecular structure, conformational energies for the isomers formed by the rotation around the single bond between C and D ring, were calculated. To discuss the effect of the single bond rotation we will obtain the potential energy curves and first transition wavelengths for two stable conformers, Pr and Pfr of **PCB**. It was observed that the potential energy curves of **PCBs** calculated by AM1 method are qualitatively similar to those found out by the *ab initio* calculations.¹⁷⁻²⁰ To obtain reliable information about conformation, we will report on a conformational analysis of **PCB** using HF/3-21G(d) and B3LYP/6-31G(d) *ab initio* calculations. We selected the HF/3-21G(d) *ab initio* method because of limitation of relatively large size of the molecules and the cost of calculations. To estimate the absorption maxima of UV spectra with respect to conformational change, the Zindo/S semiempirical method was employed. The first electronic transition energies were calculated from the Zindo/S method using the optimized geometry obtained at each computational level.²¹⁻²⁴

Methods and Computational Details

The chromophore of phytochrome protein is covalently bounded to protein *via* a thioether linkage between a cystine residue and A-ring of the open chain tetrapyrrolic chromophore. To investigate the structure and electronic properties of the chromophore, the molecule which thioether group of cysteine residue is capped into thiomethyl group are adopted as model of the open chain tetrapyrrolic chromophore (Fig. 1).²⁵⁻²⁷

To obtain the optimized structures of **PCBs**, semiempirical

AM1, PM3 methods, *ab initio* HF calculation with 3-21G(d) basis set, and DFT calculation with B3LYP/6-31G(d) are employed.²³ Structures of **Pr**, and **Pfr** isomers of **PCB** were fully optimized by starting from initial structures of various torsion angles, respectively. One of the input structures were planar between A, B, C, and D pyrrole rings ($\psi_1 = \psi_2 = \psi_3 = 0.0^\circ$). Another structures were the conformations which pyrrole rings were almost perpendicular to vinylene group ($\psi_1 = 90^\circ$, $\psi_2 = 90^\circ$, and $\psi_3 = 90^\circ$). The other structure was the conformation which phenyl groups were almost perpendicular to vinylene group ($\psi_1 = 90^\circ$, $\psi_4 = 90^\circ$, and $\psi_3 = 90^\circ$). The parameters of the optimized structures were summarized in Table 1. To investigate the stable conformational structures for the isomers, *ab initio* calculations were carried out in the Gaussian 03 package.²³ To display the potential energy curves for a variety of **PCBs**, the torsional angles (ψ_1 , ψ_2 , and ψ_3) between the pyrrole groups and the vinyl unit were fixed at optimized torsion angles. The torsion angle, ψ_3 between the pyrrole rings and the vinyl unit varies by 10 degree as shown in Figure 1 and the torsion angle was fixed while the remainder of geometrical parameters of the isomer were fully optimized. The potential energy curves according to torsion angle, ψ_3 are obtained by using semiempirical methods, *ab initio* HF, and DFT calculations.¹³

Electronic properties of the isomers are obtained by applying the optimized structures and the selected geometries (maxima or minima) of potential curves to the Zindo/S method.²¹⁻²³ The Zindo/S method including configuration integral as employed in the *Gaussian 03* package was used to calculate the singlet-singlet electronic transition energies of the optimized conformers. To investigate the change of UV spectroscopic transitions with respect to the torsion angle, the optimized structures were selected. By using the results, the dependency of conjugation for the energy gaps is analyzed. The Zindo/S method has been shown to yield reliable electronic structures for a wide variety of conjugated polymers, including those with PPV derivatives.²⁰

Results and Discussion

Equilibrium Structures of Pr and Pfr Isomers. For **Pr** and **Pfr** isomers, optimized structures of the lowest energy conformer of each is obtained by AM1 method, PM3

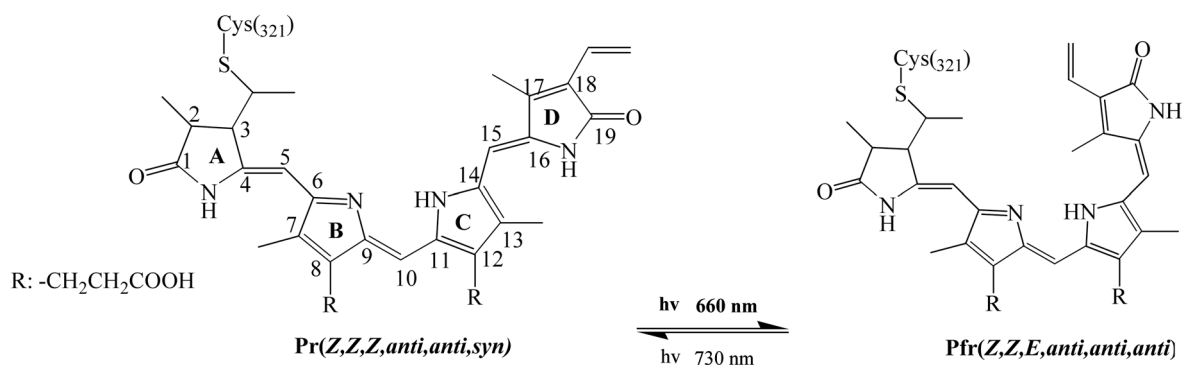


Figure 1. Structures of **Pr** and **Pfr** isomers.

method, and HF/3-21G(d) method. The bond length and torsion angles of optimized structures are given in Table 1. The atomic numbering is indicated in Figure 1. The torsion angles are displayed that $\psi_1 = \angle C4-C5-C6-N2$, $\psi_2 = \angle C9-C10-C11-N3$, $\psi_3 = \angle N3-C14-C15-C16$, $\psi_4 = \angle C14-C15-C16-C17$, respectively.

For **Pfr** isomer, the AM1 calculations are predicted that the vinyl unit is twisted by $\psi_1 = 125.0^\circ$, $\psi_2 = -2.9^\circ$, $\psi_3 = 55.7^\circ$, and $\psi_4 = -175.6^\circ$, with respect to the pyrrole ring, respectively. The energy barrier over the planar conformation is very small as shown in Table 2. The *ab initio* HF calculations for **Pfr**, support the AM1 results, producing a quit flat potential energy curve up to the torsion angles of $\psi_1 = 131.8^\circ$, $\psi_2 = 3.2^\circ$, $\psi_3 = -43.7^\circ$, and $\psi_4 = 172.0^\circ$. In optimized geometry obtained from DFT calculation, the torsion angles are given by $\psi_1 = 149.6^\circ$, $\psi_2 = -1.0^\circ$, $\psi_3 = -26.5^\circ$, and $\psi_4 = 167.8^\circ$. The pyrrole rings A is twisted to the pyrrole ring B, the pyrrole ring C is planar with respect to the pyrrole ring B, the pyrrole ring D is twisted to the pyrrole ring C. The torsion angles of **Pfr** computed at PM3, are close to the AM1 results. The PM3 equilibrium structure of **Pfr** isomer are produced a quit planar, the torsion angles are, $\psi_1 = 93.9^\circ$, $\psi_2 = 1.6^\circ$, $\psi_3 = 98.1^\circ$, and $\psi_4 = -176.8^\circ$. The pyrrole rings A is perpendicular to the pyrrole ring B, the pyrrole ring C is planar with respect to the pyrrole ring B, the pyrrole ring D is twisted to the pyrrole ring C.¹¹

In the case of **Pr** isomer, the torsion angles are considerably reasonable. the AM1 calculations are predicted that the vinyl unit is twisted by $\psi_1 = 125.0^\circ$, $\psi_2 = -2.0^\circ$, $\psi_3 = 32.5^\circ$, and $\psi_4 = 4.0^\circ$, respectively. The *ab initio* calculations for **Pr**, support the AM1 results, producing a quit flat potential energy curve up to the torsion angles of $\psi_1 = 136.3^\circ$, $\psi_2 = 6.1^\circ$, $\psi_3 = -12.0^\circ$, and $\psi_4 = -3.2^\circ$. The conformation of **Pr** isomer is predicted that the pyrrole rings A is

twisted to the pyrrole ring B, the pyrrole ring C is planar with respect to the pyrrole ring B, and the pyrrole ring D is twisted to the pyrrole ring C. The torsion angles of **Pr** computed at PM3, are different from the AM1 results. The PM3 equilibrium structure of **Pr** isomer are produced a quit planar, the torsion angles are, $\psi_1 = 73.8^\circ$, $\psi_2 = -22.4^\circ$, $\psi_3 = -1.2^\circ$, and $\psi_4 = -3.7^\circ$. In optimized geometry obtained from DFT calculation, the torsion angles are given by $\psi_1 = 152.8^\circ$, $\psi_2 = -1.65^\circ$, $\psi_3 = 11.5^\circ$, and $\psi_4 = 3.8^\circ$. The pyrrole rings A is perpendicular to the pyrrole ring B, the pyrrole ring C is planar with respect to the pyrrole ring B, the pyrrole ring D is twisted to the pyrrole ring C.

Gorb *et al.* reported conformational analysis results for dipyrrolic compound, pyromethenone by using AM1, PM3, HF/3-21G(d), and B3LYP/6-31G(d) methods.¹¹⁻¹³ The results for AM1 method were in qualitative are agreement with HF method. The torsion angles of **Z,syn** and **Z,anti** conformers were 150° - 159° , 30° , respectively. The torsion angles of **E,syn** and **E,anti** conformers were 145° - 147° , 36° - 42° , respectively.

For **Pr** and **Pfr** isomers, the single bond lengths in conjugated backbone for *ab initio* HF calculation are longer than that for AM1 calculation. However, the double bond length of the group in *ab initio* calculation is shorter than the length from AM1 result. Finally, in *ab initio* calculation the bond alternations are 0.151-0.160 Å and in the case of AM1 result the alternations are 0.108-0.113 Å. The differences for the bond alternation with respect to calculation methods affect in the obtained optical properties for **Pr** and **Pfr** isomers. The effect of the bond alternation in optical properties will be discussed later.

Conformational Analysis of Pr and Pfr Isomer. Recently, conformational analysis of organic molecules as the model for **PCBs** have been carried out from *ab initio* calculations

Table 1. Optimized geometric parameters of **Pr** and **Pfr** isomers. Bond lengths (Angstrom) and torsion angles (degree)^d

Parameters	Pfr				Pr			
	AM1	PM3	HF ^b	DFT ^c	AM1	PM3	HF	DFT
Bond length (Å)								
C4-C5	1.349	1.342	1.322	1.352	1.340	1.342	1.323	1.323
C5-C6	1.451	1.456	1.466	1.456	1.451	1.453	1.459	1.452
C6-N2	1.329	1.326	1.295	1.332	1.322	1.325	1.296	1.334
N2-C9	1.433	1.445	1.417	1.390	1.446	1.448	1.417	1.391
C9-C10	1.355	1.349	1.342	1.393	1.320	1.350	1.343	1.384
C10-C11	1.430	1.429	1.424	1.414	1.430	1.432	1.431	1.418
C11-N3	1.388	1.392	1.370	1.421	1.395	1.398	1.364	1.372
N3-C14	1.442	1.450	1.354	1.404	1.389	1.392	1.354	1.364
C14-C15	1.432	1.435	1.456	1.422	1.425	1.436	1.445	1.429
C15-C16	1.352	1.344	1.330	1.369	1.345	1.347	1.332	1.369
Torsion angles								
ψ_1	125.0	93.9	131.8	149.6	125.0	73.8	136.3	152.8
ψ_2	-2.9	1.6	3.2	-1.0	-2.0	-22.4	6.1	-1.6
ψ_3	55.7	98.1	-43.7	-26.5	32.5	-1.2	-12.0	11.5
ψ_4	-175.6	-176.8	172.0	167.8	4.0	-3.7	-3.2	3.8

^aTorsion angles: $\psi_1 = \angle C4-C5-C6-N2$; $\psi_2 = \angle C9-C10-C11-N3$; $\psi_3 = \angle N3-C14-C15-C16$; $\psi_4 = \angle C14-C15-C16-N4$. ^bOptimized structure from HF calculation with 3-21G(d) basis set. ^cOptimized structure from DFT calculation with 6-31G(d) basis set.

using a various of basis sets.^{11,12} For the methoxy-substituted thiophene oligomers, Dicesare *et al.* reported that the HF/3-21G(d) and HF/6-31G(d) basis sets give identical potential energy surface with similar energy barriers and minima.²⁸ We have used the HF/3-21G(d) method as the more elaborated calculation in this paper to have reasonable calculation times and because this basis set gives similar result in comparison with more elaborated basis sets. Potential energy curves of the **Pr** and **Pfr** isomers of PCB molecule are obtained by *ab initio* HF/3-21G(d) and DFT/6-31G(d) as well as semiempirical calculation as shown in Figures 2 and 3. The energies and torsion angles of the minima and maxima of each molecule as obtained by semiempirical, HF/3-21G(d), and B3LYP/6-31G(d) methods are displayed in Table 2.

In optimized structures, the torsion angles between pyrrole ring (B) and vinylene group adjoining pyrrole ring (A) are around 120°, but not planar. The *p*-orbitals of B-ring are perpendicular to the *p*-orbitals of vinylene carbons, so that the resonance structure between B-ring and vinylene carbons may not expected. The optimized structures of **Pfr** and **Pr** isomers are given torsion angle (ψ_1) of 131.8° and 136.3° by using HF/3-21G(d) basis set, respectively. The torsion angles between pyrrole ring (C) and vinylene group adjoining pyrrole ring (B) are around 0°. The *p*-orbitals of B-ring are planar to the *p*-orbitals of vinylene carbons, so that the resonance structure between B-ring and vinylene carbons may expected. The optimized structures of **Pfr** and **Pr** isomers are given torsion angle (ψ_2) of 3.2° and 6.1° by using 3-21G(d) basis set, respectively. The torsion angles between pyrrole ring (C) and vinylene group adjoining pyrrole ring (D) are twisted. The *p*-orbitals of C-ring are planar to the *p*-orbitals of vinylencarbons, so that the resonance structure between C-ring and vinylene carbons may expected. The optimized structures of **Pfr** and **Pr** isomers are given torsion angle (ψ_3) of -43.7° and -12.0° by using 3-21G(d) basis set, respectively. For **Pfr** and **Pr** isomers, *syn* conformers are more favorable than the anti conformers. *Syn* conformers can not exist due to steric hinderance between methyl group in C pyrrole ring and N-H group in D ring.^{11,13,29} However conformers can be experienced steric hinderance between methyl group in C pyrrole ring and methyl group in D ring. The energy difference between *syn* conformers and twisted conformers is small. In partial, the energy for *syn* conformers of **Pr** isomer almost equal to twisted conformer. The HF/3-21G(d) results give that the barrier between *syn* conformer and twisted conformer in **Pfr** and **Pr** isomers are 3.77 and 0.98 kcal/mol, respectively.

For the conformation analysis of the **Pfr** and **Pr** isomers, the twisted conformers are more stable than the coplanar structure because of the steric repulsion. The potential energy curves of **Pr** are displayed in Figure 2. It is clear that the HF/3-21G(d) result gives higher rotational energy barrier than AM1 and PM3 results. However, the potential energy surfaces obtained from semiempirical PM3 method is not considerably realistic.^{14,15} The rotational energy barrier from B3LYP/6-31G(d) result is higher than HF/3-21G(d) result.

The minimum were coplanar conformation where we expect some steric hinderance, even though the potential maximum is similar to that of the AM1 method. The potential energy curves for **Pr** isomer are very similar with respect to each calculation method.

Ab initio calculations performed at the HF/3-21G(d) level show that the most stable conformations of **Pr** isomer corresponds to twist structures with torsion angles around -12.0° as shown in Figure 2. From the result for HF method the twisted conformers of **Pr** isomer are found to be more stable than the anti conformation by 11.68 and stable than the *syn* conformation by 1.00 kcal/mol, respectively, as shown in Table 2. The perpendicular conformer is higher barrier than twist conformer by 8.72 kcal/mol. In the case of B3LYP/6-31G(d), the twisted conformers of **Pr** isomer are found to be more stable than the anti conformation by 7.23, and stable than the *syn* conformation by 0.43 kcal/mol, respectively, The perpendicular conformer is higher barrier than twist conformer by 7.48 kcal/mol. Two factors are involved in the

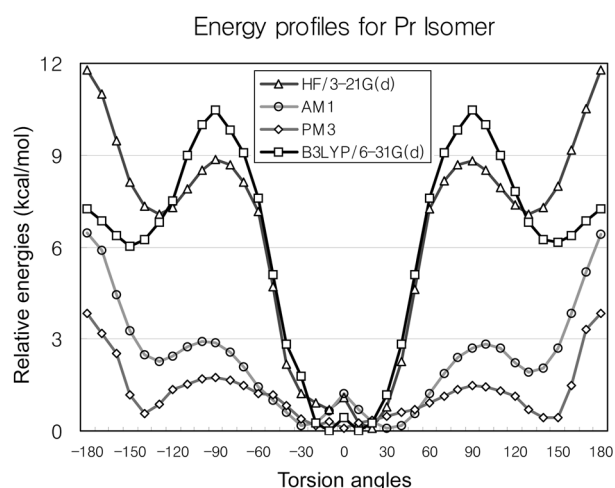


Figure 2. *Ab initio* HF/3-21G(d), B3LYP/6-31G(d), PM3, and AM1 potential energy curves for **Pr** isomer. Torsion angles of pyrrole groups(C-D rings) are varied with ψ_3 .

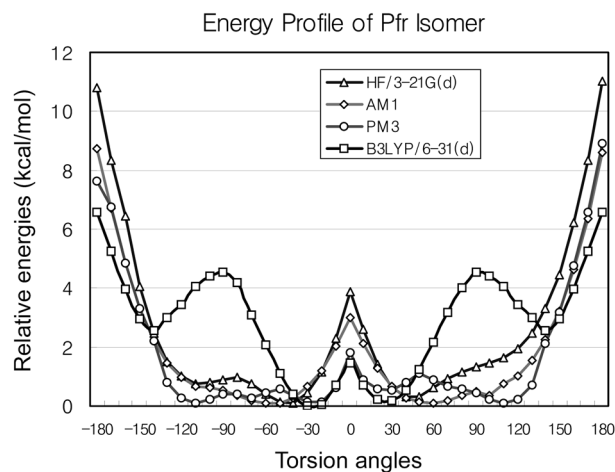


Figure 3. *Ab initio* 3-21G(d), B3LYP/6-31G(d), PM3, and AM1 potential energy curves for **Pfr** isomer.

Table 2. Relative energies (ΔE , kcal/mol) and torsion angles (degree) at the C-D ring for minimum energy and transition structures of **Pr** and **Pfr** isomers

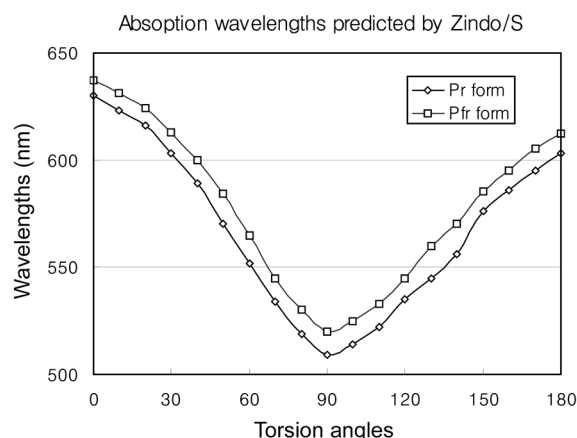
Structures		Methods			
		AM1	PM3	HF/ 3-21G(d)	BLYP/ 6-31G(d)
Pfr (<i>twist I</i>) ^a	ΔE	0.0	0.0	0.0	0.0
	ψ_3	55.7	-20.0	-43.7	-26.5
Pfr (<i>twist II</i>) ^b	ΔE	-	0.0	-	2.54
	ψ_3	-	98.1	-	150.0
Pfr (<i>syn</i>) ^c	ΔE	2.91	1.71	3.76	1.44
Pfr (<i>perp</i>) ^d	ΔE	0.39	0.34	1.21	4.55
Pfr (<i>anti</i>) ^e	ΔE	8.49	8.79	10.86	6.55
Pr (<i>twist I</i>)	ΔE	0.0	0.0	0.0	0.0
	ψ_3	32.5	-1.2	-12.0	11.5
Pr (<i>twist II</i>)	ΔE	1.79	0.35	7.00	6.02
	ψ_3	130.0	140.0	130.0	150.0
Pr (<i>syn</i>)	ΔE	1.12	0.0	1.00	0.43
Pr (<i>perp</i>)	ΔE	1.36	1.36	8.70	10.46
Pr (<i>anti</i>)	ΔE	6.34	3.73	11.65	7.21

^a*twist I* form is the most stable conformer and $\psi_3 = \angle N_3-C_{14}-C_{15}-C_{16}$.
^b*twist II* form is the local minimum conformer between *perp* and *anti* forms.
^c*syn* form is the conformer that the torsion angle, ψ_3 is 0.0° .
^d*perpendicular* form is the conformer that the torsion angle, ψ_3 is 90.0° .
^e*anti* form is the conformer that the torsion angle, ψ_3 is 180.0° .

description for the molecular conformation of the **Pr** isomer. The steric hinderance between the hydrogen of pyrrole group and that of vinyl group, which favors twisted conformations and the π -electron conjugation along the molecular frame, which favors the planarity of the molecule. The equilibrium structures of **Pr** isomer can be considered as a compromise between these two factors. However the energy barrier between the twisted conformer and planar conformer is so small.^{11,13,14}

The potential energy curve of **Pfr** are displayed in Figure 3. At the HF/3-21(d) level the most stable conformations of **Pfr** isomer corresponds to twist structures with torsion angles around -43.7° as shown in Figure 3. From the result for HF method the twisted conformers of **Pfr** isomer are found to be more stable than the anti conformation by 10.90, and stable than the *syn* conformation by 1.22 kcal/mol, respectively, as shown in Table 2. The perpendicular conformer is higher barrier than twist conformer by 3.77 kcal/mol. In the case of B3LYP/6-31G(d), the twisted conformers of **Pr** isomer are found to be more stable than the anti conformation by 6.56, and stable than the *syn* conformation by 1.45 kcal/mol, respectively, The perpendicular conformer is higher barrier than twist conformer by 4.56 kcal/mol.

The twisted conformers of **Pfr** and **Pr** isomers in *ab initio* HF/3-21G(d) calculation are found to be far more stable than the perpendicular structure by 1.22, 8.72 kcal/mol, respectively, The rotational energy barriers between the twisted and the perpendicular conformer are much higher than those between twisted and planar conformer. The perpendicular conformers are unfavorable energetically because π -electron conjugation in the molecular frame is interrupted. The

**Figure 4.** First singlet-singlet electronic transition wavelengths (nm) of **Pr** and **Pfr** isomers predicted by Zindo/S calculation for optimized geometries at B3LYP/6-31G(d).

barriers from AM1 calculation show considerably smaller than the results by *ab initio* calculations. According to the conformational analysis of **Pfr**, the *syn* conformer which C-ring is perpendicular to D-ring are more stable than the coplanar or twist structure because of the steric repulsion of substituents. As shown in the conformational analysis of **Pfr**, the HF/3-21G(d), B3LYP/6-31G(d), and AM1 methods give similar potential energy surfaces each other.

Electronic Properties of Pr and Pfr Isomer. The first electronic transition energies were calculated from Zindo/S semiempirical method using the optimized geometry obtained at each calculation levels. For **Pr** and **Pfr** isomers, the transition wavelengths in optimized geometries are displayed in Figure 4. The transition energies are absolutely depend on the torsion angle between C and D-ring rings. The predicted λ_{\max} values for optimized **Pfr** structures are more red shifted than that for the corresponding **Pr** isomer at each torsion angle. The red shift calculated is attributed to the conjugation length of pyrrolic chain and steric hinderance of substituents.

The electronic transition energies from Zindo/S calculation strongly depend on the optimized geometric parameters in the calculations for the same torsional angle. In fact, transition energies for optimized structures from semiempirical AM1 and PM3 methods are smaller than those for geometries optimized at *ab initio* calculation. Each geometrical parameter may influence the transition energies obtained by Zindo/S calculation.^{22,23} For methoxy-substituted bithiophene system, DiCesare *et al.* reported that the structure calculated from *ab initio* method gives the methoxy groups as twisted relatively to the molecular frame, whereas in the structure from semiempirical methods methoxy groups placed in coplanar with the rest of the molecule.²⁸

However, the transition energies for **Pr** isomer are displayed the same tendency as **Pfr** isomer in our calculation. To find another geometrical factor for the transition energy, we have investigated the effect of the bond alternation of vinylene linker group for each calculation. It was mentioned

Table 3. Zindo/S results for electronic transition wavelengths(nm) of **Pr** and **Pfr** isomers for optimized structures by using *ab initio* HF/3-21G(d) and AM1 methods

Isomers	Method	<i>syn</i>	<i>twist</i> ^a	<i>perpend</i> ^b	<i>anti</i>
Pfr	HF/3-21G(d)	536	528	449	506
	B3LYP/6-31G(d)	630	601	529	607
Pr	HF/3-21G(d)	527	495	452	506
	B3LYP/6-31G(d)	639	631	509	603

^aThe transition wavelengths at angles given in Table 2. ^bThe transition wavelengths at angle, $\psi_3 = 90^\circ$.

in equilibrium geometries that the bond alternation of the structure optimized at the HF/3-21G(d) method gives larger than that of the structure from semiempirical methods. It is indicated that the result of AM1 calculation give more conjugate geometry than *ab initio* calculation.

For each calculation method used to obtain optimized geometries, the absorption wavelength is considerably different. However, the wavelength decreases as the molecule becomes more twisted. This tendency is well known and is due to decrease in the overlap between p_z orbitals of carbon atoms in the phenyl ring and vinyl group as the torsional angle increase. This induces to a reduction in the electronic conjugation length and an increase in the electronic transition energy,²⁰

$$\lambda_{\max}(\text{Predict}) = \lambda_0 - \Delta\lambda/2 (\sin\phi + \sin^2\phi),$$

where λ_0 is the absorption wavelength of optimized geometry at torsion angle, $\phi = 0^\circ$, and $\Delta\lambda$ is the difference between the absorption wavelengths at 90° and 0° .

The absorption wavelengths at the potential minima (or maxima) for **Pr** and **Pfr** isomers are shown in Table 3. The absorption wavelengths are calculated at optimized geometry from HF/3-21G(d) and B3LYP/6-31G(d) level. The wavelengths from B3LYP/6-31G(d) geometries are larger than the values from HF/3-21G(d). However, it is shown that electronic properties of the isomers strongly depend on the planarity of pyrrole groups and vinylene groups.

The planarity between vinylene and phenyl group is affected to produce the changes in electronic properties.^{4,6,7} HOMO-LUMO gaps are small by increasing the planarity. At a torsion angle of 90° , the energy gaps of the conjugated systems increase to maximum due to the reduced π overlap between the phenyl ring and the vinylene unit. Since the interaction between the phenyl rings and the vinylene unit is antibonding in HOMO and bonding in the LUMO, the reduction of π overlap stabilizes the HOMO level, but destabilizes the LUMO level. The degree of the stabilization of the HOMO energy level is smaller in energy than the destabilization of the LUMO energy level.^{6,7} For **Pr** and **Pfr** isomers the wavelength, λ_{\max} values according to change of conformations are predicted as shown in as shown in Figure 4.

In summary, the potential energy curves in **Pr** and **Pfr** isomers are different shapes each other in building block of **PCB** molecule, including the vinyl groups and pyrrole

groups. However, the curves for each isomer in according to calculation method are similar shape. It is shown that the steric repulsion interactions between pyrrole ring and vinyl group are subjected to similar type. For the fully conjugate molecules, λ_{\max} values according to change of conformations will changes because of the steric repulsion interaction and the difference of π -conjugation.

Conclusion

Structures of **Pr** and **Pfr** isomers of **PCB** chromophore of phytochrome were optimized and conformational analysis for the isomers are performed in semiempirical and *ab initio* method. As shown in Figure 2 and 3, the potential energy curves of two isomers are shown symmetric shape about planar conformation. In **Pr** isomer, semiempirical result are different from *ab initio* methods. The potential energy surfaces predicted by AM1 and *ab initio* methods are quite shallow around the planar conformations ($-40^\circ \sim 40^\circ$). The energy barrier of perpendicular conformers are less than 3.0 kcal. However, The HF and DFT results for **Pr** isomer are shown that the energy barrier of perpendicular conformers come up to 8.72 and 10.48 kcal/mol, respectively. For potential energy curves of **Pfr** isomer, DFT result are different from semiempirical and HF results. Semiempirical and HF result the energy barrier of perpendicular conformers are not exist. In DFT calculation the energy barrier of perpendicular conformers are about 4.56 kcal/mol.

This fact results from the compromise between two factors, a repulsion interaction and a π -conjugation effect. The repulsion interaction is mainly attributed to the short distances between hydrogen atoms on the pyrrole and the vinylene unit for **PCB**. However, in the case of **Pfr** isomer, there are repulsion not only between methyl group in C-ring and methyl group in D-ring, but also between hydrogen atoms on the C-pyrrole ring and methyl group in D-ring. In the planar conformer of **Pfr** isomer, the distances are too short compared to the sum of the van der Waals radii. The π -conjugation effect results from the fact that the large overlap between the π orbitals of C atoms linking between the pyrrole and the vinylene units gives stable conformation. For **Pr** isomer, there can not be repulsion between methyl group in C-ring and methyl group in D-ring, and between hydrogen atoms on the C-pyrrole ring and methyl group in D-ring. In the planar conformer of **Pr** isomer, it is stabilized by π -conjugation effect. Although the small rotation barrier are experienced in **Pr** isomer, the perpendicular conformer of **Pr** isomer is more stable than **Pfr** isomer.

The electronic transition energies from Zindo/S calculation strongly depend on the optimized geometric parameters in the calculations for the same torsional angle. In fact, transition energies for optimized structures from semiempirical AM1 and PM3 methods are smaller than those for optimized geometries from *ab initio* HF and DFT calculation. Although the predicted UV absorption wavelengths are not quantitatively equal to experimental data, the results are similar qualitatively. It should be considered that solvent effect and

the interactions between chromophore and phytochrome protein residues in order to explain the exact result.

Acknowledgments. This work was supported by grant (Grant No. R05-2003-000-12034-0) from the Basic Research Program of the Korea Science and Engineering Foundation. The author is grateful to the Computer Center of Chonbuk National University for the use of their computing facilities.

References

- (a) Eichenberg, K.; Baeurle, I.; Paulo, N.; Sharrock, R. A.; Ruediger, W.; Schaefer, E. *FEBS Letts.* **2000**, *470*, 107. (b) Quail, P. H. *Annu. Rev. Genet.* **1995**, *25*, 389.
- (a) Kneip, C.; Mosley, D.; Hildebrandt, P.; Gartner, W.; Braslavsky, S. E.; Schaffner, K. *FEBS Letts.* **1997**, *414*, 23. (b) Kneip, C.; Schlamann, W.; Hildebrandt, P.; Braslavsky, S. E.; Schaffner, K. *FEBS Letts.* **2000**, *482*, 256. (c) Matysik, J.; Hildebrandt, P.; Schlamann, W.; Braslavsky, S. E.; Schaffner, K. *Biochemistry* **1995**, *34*, 10497.
- Schmidt, P.; Westphal, U. H.; Worm, K.; Braslavsky, S. E.; Gartner, W.; Schaffner, K. *J. Photochem. Photobiol. B: Biology* **1996**, *34*, 73.
- Wagner, J. R.; Brunzelle, J. S.; Forest, K. T.; Vierstra, R. D. *Nature* **2005**, *438*, 325.
- Foerstendorf, H.; Mummert, E.; Schaefer, E.; Scheer, H.; Siebert, F. *Biochemistry* **1996**, *35*, 10793.
- Kneip, C.; Hildebrandt, P.; Schlamann, W.; Braslavsky, S. E.; Mark, F.; Schaffner, K. *Biochemistry* **1999**, *38*, 15185.
- Andel, F.; Lagarias, J. C.; Mathies, R. A. *Biochemistry* **1996**, *35*, 15997.
- Borg, O. A.; Durbeej, B. *J. Phys. Chem. B* **2007**, *111*, 11554.
- von Thor, J. J.; Mackeen, M.; Kuprov, I.; Dwek, R. A.; Wormald, M. R. *Biophys. J.* **2006**, *91*, 1811.
- Evans, K.; Grossmann, J. G.; Fordham-Sketton, A.; Papiz, M. Z. *J. Mol. Biol.* **2006**, *346*, 655.
- (a) Gorb, L.; Korkin, A.; Leszczynski, J. *J. Mol. Struct. (Theochem)* **1998**, *454*, 217. (b) Gorb, L.; Korkin, A.; Leszczynski, J.; Varneck, A.; Mark, F. *J. Mol. Struct. (Theochem)* **1998**, *425*, 137.
- Marai, C. N. J.; Chass, A. A.; Doust, A. B.; Scholes, G. D. *J. Mol. Struct. (Theochem)* **2004**, *680*, 219.
- Korkin, A.; Merk, F.; Schaffner, K.; Gorb, L. *J. Mol. Struct. (Theochem)* **1996**, *388*, 121.
- Zahedi, M.; Shaabani, A.; Safari, N. *J. Mol. Struct. (Theochem)* **1998**, *452*, 125.
- Magdo, H.; Nemeth, K.; Mark, F.; Hildebrandt, P.; Schaffner, K. *J. Phys. Chem. A* **1999**, *103*, 289.
- Mroginsky, M. A.; Murgida, D. H.; Hildebrandt, P. *Acc. Chem. Res.* **2007**, *40*, 258.
- Remberg, A.; Ruddat, A.; Braslavsky, S.; Gartner, W.; Schaffner, K. *Biochemistry* **1998**, *37*, 9983.
- Lee, H. M.; Kim, J.; Kim, C. J.; Kim, K. S. *J. Chem. Phys.* **2002**, *116*, 6549.
- (a) Baik, J.; Kim, J.; Kim, K. S. *J. Chem. Phys.* **1999**, *110*, 9116. (b) Majumdar, D.; Kim, J. *J. Chem. Phys.* **2000**, *112*, 101. (c) Majumdar, D.; Kim, K. S. *J. Chem. Phys.* **2000**, *113*, 5259. (d) Lee, H. M.; Kim, K. S. *J. Chem. Phys.* **2001**, *114*, 461.
- (a) Kim, C. J. *Bull. Korean Chem. Soc.* **2002**, *23*, 330. (b) Hong, S. Y.; Marynick, D. S. *Macromolecules* **1992**, *25*, 3591.
- Ridley, J.; Zerner, M. C. *Theor. Chim. Acta* **1973**, *32*, 111.
- Zerner, M. C.; Loew, G. H.; Kirchner, R. F.; Mueller-Westerhoff, U. T. *J. Am. Chem. Soc.* **1980**, *102*, 589.
- Frisch, M. J.; Trucks, G. W.; Schlegel, H. B.; Scuseria, G. E.; Robb, M. A.; Cheeseman, J. R.; Montgomery, J. A., Jr.; Vreven, T.; Kudin, K. N.; Burant, J. C.; Millam, J. M.; Iyengar, S. S.; Tomasi, J.; Barone, V.; Mennucci, B.; Cossi, M.; Scalmani, G.; Rega, N.; Petersson, G. A.; Nakatsuji, H.; Hada, M.; Ehara, M.; Toyota, K.; Fukuda, R.; Hasegawa, J.; Ishida, M.; Nakajima, T.; Honda, Y.; Kitao, O.; Nakai, H.; Klene, M.; Li, X.; Knox, J. E.; Hratchian, H. P.; Cross, J. B.; Bakken, V.; Adamo, C.; Jaramillo, J.; Gomperts, R.; Stratmann, R. E.; Yazyev, O.; Austin, A. J.; Cammi, R.; Pomelli, C.; Ochterski, J. W.; Ayala, P. Y.; Morokuma, K.; Voth, G. A.; Salvador, P.; Dannenberg, J. J.; Zakrzewski, V. G.; Dapprich, S.; Daniels, A. D.; Strain, M. C.; Farkas, O.; Malick, D. K.; Rabuck, A. D.; Raghavachari, K.; Foresman, J. B.; Ortiz, J. V.; Cui, Q.; Baboul, A. G.; Clifford, S.; Cioslowski, J.; Stefanov, B. B.; Liu, G.; Liashenko, A.; Piskorz, P.; Komaromi, I.; Martin, R. L.; Fox, D. J.; Keith, T.; Al-Laham, M. A.; Peng, C. Y.; Nanayakkara, A.; Challacombe, M.; Gill, P. M. W.; Johnson, B.; Chen, W.; Wong, M. W.; Gonzalez, C.; Pople, J. A. *Gaussian 03*, revision B.05; Gaussian, Inc.: Wallingford, CT, 2003.
- Gervasio, L.; Gardini, M.; Salvi, R.; Schettino, V. *J. Phys. Chem. A* **1998**, *102*, 2131.
- Boruck, B.; van Stetten, D.; Seibeck, S.; Lamparter, T.; Michael, N.; Mroginski, M. A.; Otto, H.; Murgida, D. H.; Heyn, M. P.; Hildebrandt, P. *J. Biol. Chem.* **2005**, *280*, 34358.
- Mora, M. E.; Bar, S. E.; Awruch, J.; Delfino, J. M. *Bioorganic & Med. Chem.* **2003**, *11*, 4661.
- Koglin, M.; Behrends, S. *Biochem. Pharm.* **2002**, *64*, 109.
- (a) Belletete, M.; Mazerolle, L.; Desrosiers, N.; Leclere, M.; Durocher, G. *Macromolecules* **1995**, *28*, 8587. (b) Dicesare, N.; Belletete, M.; Leclere, M.; Durocher, G. *J. Mol. Struct. (Theochem)* **1999**, *467*, 259. (c) Dicesare, N.; Belletete, M.; Raymond, F.; Leclere, M.; Durocher, G. *J. Phys. Chem.* **1997**, *A101*, 776. (d) Dicesare, N.; Belletete, M.; Leclere, M.; Durocher, G. *J. Phys. Chem.* **1998**, *A102*, 5142.
- Kneip, C.; Hildebrandt, P.; Schlamann, W.; Nemeth, K.; Mark, F.; Schaffner, K. *Chem. Phys. Lett.* **1999**, *311*, 479.
- Dabbagh, H. A.; Chemahini, A. R. N.; Madaresi-Alam, A. R. M. *Bull. Korean Chem. Soc.* **2005**, *26*, 1229.
- Lee, M. J.; Kim, D. H. *Bull. Korean Chem. Soc.* **2006**, *27*, 39.
- (a) Staub, J. M.; Deng, X.-W. *Photochem. Photobiol.* **1996**, *64*, 897. (b) Smith, H. *Annu. Rev. Plant. Physiol. Mol. Biol.* **1995**, *167*, 330. (c) Schmidt, P.; Westphal, U. H.; Worm, K.; Braslavsky, S. E.; Gartner, W.; Schaffner, K. *J. Photochem. Photobiol. B: Biology* **1996**, *34*, 73.
- (a) Buchler, R.; Hermann, G.; Lap, D. V.; Rentsch, S. *Chem. Phys. Lett.* **1995**, *233*, 514. (b) Tokutomi, S.; Sugimoto, T.; Mimuro, M. *Photochem. Photobiol.* **1992**, *56*, 542.
- Jang, S.; Jin, S. I.; Park, C. R. *Bull. Korean Chem. Soc.* **2007**, *28*(12) 2343.